HHS Public Access

Author manuscript

NMR Biomed. Author manuscript; available in PMC 2015 June 14.

Published in final edited form as:

NMR Biomed. 2014 March ; 27(3): 291–303. doi:10.1002/nbm.3062.

Time-dependent effects of isoflurane and dexmedetomidine on functional connectivity, spectral characteristics, and spatial distribution of spontaneous BOLD fluctuations

Matthew Evan Magnuson, **Garth John Thompson**, **Wen-Ju Pan***, and **Shella Dawn Keilholz***

Georgia Institute of Technology and Emory University Biomedical Engineering, Atlanta, GA, USA

Abstract

Anesthesia is often necessary to perform fMRI experiments in the rodent model; however, commonly used anesthetic protocols may manifest changing brain conditions over the duration of the study. This possibility was explored in the current work. Eleven rats were anesthetized with 2% isoflurane anesthesia; four rats were anesthetized for a short period (30min, simulating induction and fMRI setup) and seven rats were anesthetized for a long period (3 h, simulating surgical preparation). Following the initial anesthetic period, isoflurane was discontinued, and a dexmedetomidine bolus (0.025 mg/kg) and continuous subcutaneous infusion (0.05 mg/kg/h) were administered. Blood-oxygen-level dependent resting state imaging was performed every 30 min from 0.75 h post dexmedetomidine bolus until 5.75 h post-bolus. Evaluation of power spectra obtained from time courses in the primary somatosensory cortex revealed, in general, a monotonic increase in low-frequency power (0.05–0.3 Hz) in both groups over the duration of resting state imaging. Greater low-band spectral power (0.05–0.15 Hz) is present in the short isoflurane group for the first 2.75 h, but the spectra become highly uniform at 3.25 h. The emergence of a ~0.18 Hz peak, beginning at the 3.75 h time point, exists in both groups and evolves similarly, increasing in strength as the duration of dexmedetomidine sedation (and time since isoflurane cessation) extends. In the long isoflurane group only, bilateral functional connectivity strengthens with anesthetic duration, and correlation is linearly linked to low-band spectral power. Convergence of connectivity and spectral metrics between the short and long isoflurane groups occurs at ~3.25 h, suggesting the effects of isoflurane have subsided. Researchers using dexmedetomidine following isoflurane for functional studies should be aware of the duration specific effects of the pre-scan isoflurane durations as well as the continuing influences of long-term imaging under dexmedetomidine.

Keywords

dexmedetomidine; resting-state fMRI; BOLD; physiology; power spectra; functional connectivity; spatiotemporal dynamics; isoflurane

*Correspondence to: W.-J. Pan and S. D. Keilholz, Georgia Institute of Technology and Emory University, Biomedical Engineering, Atlanta, GA, USA., wpan5@emory.edu; shella.keilholz@bme.gatech.edu.

SUPPORTING INFORMATION

Additional supporting information may be found in the online version of this article at the publisher's web-site.

INTRODUCTION

Animal models are a powerful tool, allowing for the detailed and often invasive investigation into analogues of human disease, structure, and function. Animal models have provided an ideal platform to study the origin and functions of the blood-oxygen-level dependent (BOLD) signal and functional connectivity in fMRI; however, one complication is that anesthesia is commonly required to prevent movement and alleviate pain or anxiety. In BOLD fMRI using rodents, anesthesia is almost always used, but it introduces confounding influences to the function of the neural and vascular architecture of the brain (1–7). Anesthesia directly affects basal neuronal activity as well as the coupling between neurons and the vasculature (8), so understanding an anesthesia's effect on neural activity and BOLD data is vital for interpreting functional MRI data.

Isoflurane is commonly used to induce anesthesia, perform surgical procedures, and maintain a deep level of unconsciousness in rodents during setup for fMRI (5–7,9,10). Anesthesia is typically switched to an agent that is less suppressive of neural activity for the imaging portion of the experiment, although isoflurane has been used during imaging as well (11–13). Isoflurane's anesthetic mechanism is not well understood, but it is known that is acts on GABA receptors, potassium channels, and the GLT1/EAAT2 glial glutamate transporter, resulting in complex interrelationships producing the desired anesthetic state (14). At high isoflurane doses (>1.8%) widespread cortical neural burst suppression results in reduced cortical excitation (14,15) and reduced spatial sensitivity of functional connectivity (13), while at lower dosages (<1.5%) functional activity and connectivity remain fairly intact (11–13,16). It has been demonstrated that it takes nearly an hour following isoflurane discontinuation for the end tidal volumes of isoflurane to drop below 0.1% following relatively short isoflurane paradigms (17). This residual isoflurane likely introduces lingering effects on both neural activity (continued neural suppression) and the vasculature (continued vasodilation) that must be considered.

Dexmedetomidine is a α_2-adrenergic receptor agonist which selectively binds to and stimulates α_2-adrenergic receptors after crossing the blood-brain barrier. It is also a vasoconstrictor (18,19). Dexmedetomidine acts by inhibiting adenylyl cyclase activity, causing a reduction of firing rates of locus cereleus noradrenergic neurons, thus leading to sedation (20). Unlike many other anesthetics, which deeply suppress central nervous system (CNS) activity (21), dexmedetomidine induces a neural state very similar to natural sleep (20) while simultaneously causing muscular relaxation. The drug was previously formulated as medetomidine, which contains the active enantiomer, dexmedetomidine, used in the current experiment. (In 2009, Pfizer discontinued medetomidine (Domitor) in their veterinary line and switched to dexmedetomidine (Dexdomitor)). The two drugs have nearly identical effects on the rodent; however, the dosing of dexmedetomidine is half that of medetomidine (22).

α-chloralose was once the anesthetic of choice for fMRI studies, allowing for well preserved brain activity and neurovascular coupling (1,23–25); however, the experimental setup was complicated and the experiments terminal. In 2006, Weber *et al.* presented a protocol using medetomidine sedation allowing for longitudinal fMRI studies to be performed in rats (10).

Weber's protocol provided long-term stable physiological conditions, a reproducible and expected BOLD response to forepaw stimulation (matching previous α-chloralose studies), adequate sedation, simple subcutaneous administration, and finally a quick reversal and full recovery of the rodent following experimentation. This was a drastic improvement over previously accepted protocols, allowing for longitudinal studies of fMRI in the rodent model. Following Weber's work, Pawela *et al.* released a study pointing to the advantages of stepping up the anesthetic dosage two hours after the initial bolus in order to maintain stable physiology and neural responsiveness (5). Pawela *et al.* examined the anesthetic dose dependence of both BOLD response to forepaw stimulation at several frequencies and resting state seed based functional connectivity (5). They determined that increasing the medetomidine dosage threefold approximately 2.5 h after the initial bolus preserved the frequency dependent stimulation BOLD responses and the strength of resting state functional connectivity.

In 2005, Austin *et al.* published data indicating that the BOLD response to a fixed stimulus was variable as a function of time under α-chloralose anesthesia (following halothane induction); specifically, the spatial extent and peak amplitude response to the stimulus both increased several hours post α-chloralose induction (26). Austin *et al.* suggest that changes in the BOLD response under α-chloralose were a product of combined effects of halothane and α-chloralose on neuronal activity or changes in vascular response and neurovascular coupling as a result of anesthesia. If the changes observed are related to changes in vascular tone, then variations in the BOLD response over time would theoretically manifest in spontaneous brain activity.

Slow fluctuations in the BOLD signal (presumed to be linked to spontaneous neural activity) have been used to map functional connectivity, a term used to describe spectrally and temporally coherent activity arising in different areas of the brain (2,6,7,27,28). The frequency of the fluctuations depends on the type of contrast (2) and the anesthetic agent (29). Spatiotemporal dynamic analysis reveals patterns of quasiperiodic (periodic, but not constant), often bilaterally symmetric, spatially propagating patterns of functional activity observed both in humans (30,31) and in the anesthetized rat (29,31). In the work presented here, we evaluate the time-sensitive effects of dexmedetomidine anesthesia (following initial administration of isoflurane anesthesia) on traditional functional connectivity MRI (fcMRI), the frequency specific signatures of the BOLD fluctuations, and the occurrence of spatiotemporal dynamics.

In previous experiments using (dex)medetomidine, our laboratory has observed time-dependent effects of medetomidine on functional connectivity measured with resting state fMRI, functional network spatiotemporal dynamics (29,30), and spectral characteristics of functional time courses. Consequently, we designed a longitudinal experimental paradigm using two anesthetic regimens, one with a short duration of isoflurane (30min; comparable to typical studies using isoflurane for induction and setup (5,10,16)) prior to functional imaging and another with a long isoflurane duration (3 h; comparable to studies involving complex surgical procedures such as combined electrophysiology–fMRI (3)) prior to imaging. Both paradigms are followed by an identical dosage of dexmedetomidine anesthesia concurrent with a 5.75 h imaging series.

The goal of this work is twofold: first to evaluate possible lingering, duration dependent effects of isoflurane on functional connectivity, and second to evaluate evolving changes in the rat's functional state based upon long-term use of dexmedetomidine anesthesia. We found that an extended isoflurane paradigm will attenuate functional activity for a longer duration as compared with a shorter isoflurane paradigm. Furthermore, we also observed a significant evolution of functional metrics as a result of long durations of dexmedetomidine use under the currently accepted and refined dexmedetomidine sedation paradigm. Using the dosing methods of Pawela *et al.*, we expand on their initial findings by focusing both on the effects of isoflurane prior to functional imaging on preceding functional activity and on time dependent effects of dexmedetomidine anesthesia on spontaneous BOLD frequency characteristics, spatiotemporal dynamics, and resting state functional connectivity metrics.

MATERIALS AND METHODS

Animal preparation and physiological monitoring

All experiments were performed following guidelines set by the Institutional Animal Care and Use Committee (IACUC). Eleven male Sprague Dawley rats (200–300 g) were anesthetized with 2% isoflurane mixed with ~1:1 oxygen and room air while undergoing experimental setup. The rat was placed in the MRI cradle and the head was secured with a bite bar and ear bars. Heart rate and blood oxygen saturation percentage were recorded with a pulse oximeter placed on the rear left paw. Body temperature was monitored with a rectal thermometer and maintained at ~37°C using an adjustable warm water pad. Respiratory rate was also monitored by using a pressure-sensitive balloon placed under the rat's chest.

Once setup was complete, the rat was left to rest in the cradle under 2% isoflurane until the total time under isoflurane reached 3 h (long isoflurane – experimental group 1) or 30 min (short isoflurane – experimental group 2). For the long isoflurane group, after 2h 30 min, isoflurane was reduced to 1.5% for 30 min before the induction of dexmedetomidine (Dexdomitor, Pfizer, Karlsruhe, Germany). The long isoflurane "wait period" was chosen to replicate our previous experiments, where it was necessary to keep the rat under isoflurane for long periods of time while surgical procedures were performed (3). The short isoflurane group replicates setup time for a rodent to be anesthetized and prepared for scanning where no surgery or complex setup is involved, but keeps time under isoflurane the same for all rats. Following the wait period, the short isoflurane group was switched directly from 2% isoflurane to dexmedetomidine.

A subcutaneous bolus injection of 0.025 mg/kg dexmedetomidine was administered subcutaneously to the rat's right rear upper leg. Five minutes after the dexmedetomidine bolus, isoflurane was discontinued. Fifteen minutes post-bolus, subcutaneous infusion of 0.05 mg/kg/h dexmedetomidine was initiated using a butterfly needle taped in place to maintain anesthetic depth for the duration of the experiment (10). Approximately 80 min following the initial dexmedetomidine bolus, the infusion dosage was increased to 0.15 mg/kg/h (3 × initial infusion rate) for maintaining anesthetic depth (5). The beginning of the threefold increased infusion did not exactly match Pawela's protocol. In experiments where surgery was performed, it was necessary to ensure anesthetic depth, and we found that

increasing the dexmedetomidine dosage at ~80min was conducive to adequate sedation with no alteration of functional activity (4,10).

Image acquisition

All resting state functional images were acquired on a 20cm horizontal bore 9.4T Bruker BioSpec magnet equipped with an actively shielded gradient coil capable of producing 20G/cm gradient strength with a rise time of 120 μs. The BioSpec was interfaced with an AVANCE (Bruker, Billerica, MA) console. An actively decoupled imaging setup was used, including a 2 cm surface coil for reception and a 7cm volume coil for RF transmission (Bruker, Billerica, MA).

A FLASH image was acquired in three planes, providing necessary anatomical information to properly position the single slice to be used for resting state imaging. Using the flash image a coronal slice was selected covering the primary somatosensory (S1) cortex, based on known anatomical markers. Shimming was conducted on this single slice to obtain maximum signal-to-noise ratio and spatial homogeneity. 45 min after the initial dexmedetomidine bolus, the first resting state scan was collected with the following parameters: Single-shot gradient echo EPI, 1000 repetitions, T_R = 500 ms, T_E = 15ms, total scan time = 8 min 20 s, number of slices = 1, slice thickness = 2 mm, FOV = 2.56 cm × 2.56 cm, matrix size = 64 × 64. Every 30 min this identical resting state scan was repeated until the 5.75 h mark was reached. This paradigm constituted a total of 11 scans; all scans were collected in eight of 11 rodents. One rodent was missing the initial time point, one rodent was missing two of the initial time points due to delays during setup, one rodent was missing the final scan, and another rodent was missing the final three scans. They were removed from the scanner early because of abnormally increased heart rate and slight motion (indicating the rat might have been coming out of sedation). Following the final scan, rodents were removed from the MRI scanner.

Data analysis

Functional activity and spectral metrics were directly compared between the short and long isoflurane experimental groups. Functional metrics were also compared between early and late portions of the experiment within each group. All fMRI data processing and analysis was performed using code written in MATLAB (MathWorks, Natick, MA). Two initial preprocessing steps were performed before data evaluation. First the mean value was subtracted from functional time courses, followed by division by one standard deviation to normalize for comparison between rats (29). Following normalization, whole brain signal regression was performed (13).

Spectral analysis—Following the initial preprocessing, spectral data were evaluated. A nine voxel (3 × 3 square) ROI from the single coronal slice imaged was chosen manually in the forepaw region of the S1 cortex, and a functional time course was obtained for the average intensity in the ROI for the duration of the scan. Power spectra were obtained for the resulting functional time course, using the Welch method (200 s sections, 99.5% overlap, Hamming window). The resulting power spectra were averaged at each time point to create a spectrum for both experimental groups, highlighting frequencies where consistent high

power is present, while reducing noise from anomalous frequency components. Maximum power value (%/cHz), maximum power frequency location (Hz), and the center of mass (CoM) for power (Hz) were calculated using spectral data between 0.05 and 0.3 Hz (chosen based on analysis of low-frequency BOLD power localization from previous works) (2,29,31). For the purposes of this manuscript, when describing spectral ranges, the designations “low-band,” “high-band,” and “broad-band” power will be used. Data were divided into low-band power (0.05–0.149 Hz), high-band power (0.015–0.30 Hz), and broadband power (0.05–0.3 Hz). Spectral data below 0.05 Hz were not used for raw spectral analysis due to the presence of high-powered 0–0.05 Hz components in some of the data sets that were not removed by detrending or global signal regression. Each set of values was plotted against dexmedetomidine sedation time to determine time sensitive systematic influences of the anesthesias.

Functional connectivity analysis—Functional connectivity and spatiotemporal dynamics were evaluated for each data set. Additional preprocessing was required before analysis; data were linearly detrended followed by FIR band pass filtering between 0.01 and 0.3 Hz (allowing for removal of DC artifacts and higher-frequency components). The ROI selected for spectral analysis was used to obtain a time course of the filtered and detrended S1 data. The functional time course of the left S1FL was then correlated with all other voxels in the image to obtain a functional connectivity map. The correlation values (r) from the 15 most highly correlated voxels in the hemisphere contralateral to the seed (clustered in S1) time course were averaged to generate a functional connectivity value for every rat and every scan. Correlation values were plotted against dexmedetomidine sedation times. Total low-band spectral power was plotted versus broadband functional connectivity to determine if a relationship exists between the two. All data points for each experimental group were plotted on a scatter plot, and R^2 (linear regression), r (Pearson correlation), and p values (unpaired, two-tailed, equal variance t-tests; multiple-comparisons corrected) were calculated for each group.

Global signal connectivity was evaluated (using processed data without global signal regression) by performing Pearson correlation between the functional time course representing the whole brain signal and all other voxels in the brain. The resulting Pearson correlation values for all brain voxels were then averaged to obtain global connectivity for each rat and scan.

Spatiotemporal dynamic analysis—A pattern-finding algorithm designed to identify reproducible spatiotemporal dynamics was applied to the filtered data (29,31), allowing for the visualization of patterns of low-frequency activity that propagate through cortical and subcortical brain regions. A chunk of consecutive images is chosen from the resting state data set at a random starting position; sliding correlation is then performed between the image chunk and the preprocessed image series, correlation peaks are detected from the sliding correlation data, and image chunks corresponding to the correlation peaks are then averaged together to create a new template. This averaged template is once again used in sliding correlation analysis; this process continues until convergence is reached. The final template, containing 11 images in this case (5.5 s), is then displayed on an image strip or as

a movie to allow for ideal viewing of spatiotemporal dynamic patterns. This algorithm is explained in detail by Majeed *et al.* (29,31).

Templates for each scan were visualized on a blue-to-red color scale (colors indicate template strength: blue – low, red – high, the "jet" colormap in MATLAB). Each template was evaluated by an experienced researcher, who classified each run as either containing or not containing spatiotemporal dynamics. Scans were grouped in a Boolean fashion as either showing or not showing the presence of spatiotemporal dynamics.

Inter- and intra-group t-tests—Two sets of statistical analyses were performed, intergroup and intragroup analysis. Unpaired, two-tailed, equal variance *t*-tests were performed between the two experimental groups (short and long isoflurane exposure) at each time point for all metrics discussed above (except spatiotemporal dynamics). Unpaired, two-tailed, equal variance *t*-tests were also performed within each experimental group comparing data from the first half of the imaging series (0.75–3.25 h) with data from the second half of the imaging series (3.75–5.75 h) to evaluate evolving properties of each metric. This division of time points was chosen because of the emergence of the ~0.18 Hz peak at this time point; in addition, it represents the half-way point of functional imaging.

Multiple regression analysis: resting state metrics and physiology—Multivariate ANOVA analysis was performed to determine if quantified functional resting state metrics were significantly coupled with variation in physiological parameters. Heart rate was obtained in nine out of 11 rats, oxygen measurements were collected in 10 out of 11 rats, and breath rate and temperature were collected for all 11 rats. For each rat, spectral CoM, maximum power, frequency location of maximum power, bilateral connectivity, and total low-frequency power (0.05–0.3 Hz) were independently evaluated versus all physiological recordings (heart rate, breath rate, blood oxygen, and body temperature). Four *p*-values were obtained for each ANOVA, indicating the statistical significance and interaction effects of the relationship between all physiological parameters and the evaluated functional resting state metrics (spectral CoM, maximum spectral power, frequency location of maximum spectral power, maximum connectivity, and total spectral power between 0.05 and 0.3 Hz). Multiple regression ANOVAs were performed for each rodent's physiological parameters and each calculated resting state (RS) metric (a total of 50 ANOVAs). Twenty sets of *p*-values were obtained (five functional metrics × four physiological parameters).

Inter-group physiological parameters were examined to determine if there was a difference in physiology between the short and long isoflurane groups. Physiological values were averaged together for all rats to determine if physiological condition shifted significantly over the course of the experiment. Student *t*-tests were performed comparing physiological data from the first half of the experiment (0.75–3.25 h) to the same parameters from the second half of the experiment (3.75–5.75 h).

Correcting for multiple comparisons—The sequential goodness of fit (SGoF) method developed by Carvajal-Rodriguez *et al.* (32) was used to correct for multiple comparisons to control the chance that false positives would be considered significant. Seventy-seven hypotheses were tested regarding the relationship between our two experimental groups

(seven functional metrics on 11 different time points). SGoF performs a binomial test based on a null hypothesis on the expected distribution of the *P*-value family created from the 77 Student *t*-tests performed. This controls the chance of false positives being presented (type 1 errors) to a set value, but does not increase the change for false negatives (type 2 errors) as much as Bonferroni or false-discovery rate controlling methods (32). SGoF was also performed on a second family of hypotheses (intra-individual comparisons), where data from the first six time points for each rat are compared with the next five time points to test for significant differences. Eight comparisons are made for both experimental groups for a total of 16 comparisons. All values described as significant in the results section have passed SGoF multiple-comparison correction at 0.05.

RESULTS

All components of functional network activity explored in this study exhibited evolving properties occurring as length of time from isoflurane use increased and the duration of dexmedetomidine exposure increased. Each time point evaluated consists of data from 11 rats excluding the 0.75 h time point (nine rats), the 1 h time point (10 rats), the 4.75 and 5.25 h time points (10 rats), and the 5.75 h time point (nine rats). Data were not collected from all rats for these data points and are explained in detail in the methods section. A summary of all inter- and intra-subject statistical comparisons can be found in Table 1 and Table 2 respectively; all values highlighted in bold are significant and have passed SGoF multiple-comparison correction at a threshold of 0.05 (Table 1, $p < 0.0319$; Table 2, $p < 0.0345$).

Spectral characteristic evolution

Inter-group analysis—Figure 1 contains the group average of spectral components obtained from time courses extracted from the right primary somatosensory area for the forelimb (S1FL) at each recorded time point for both short and long isoflurane groups. Data collection began 0.75 h following the initial dexmedetomidine bolus. Resting state scans occurred at 30min intervals until the 5.75 h post-bolus data point is reached (11 plots represent 11 time points).

At the 0.75 h time point, power is low across the entire spectrum; slightly higher power exists in the low-frequency band. (0.05 Hz–0.149 Hz) for both experimental groups. At the second time point (1.25h), the short isoflurane group displays a major increase in low-frequency power; low-frequency power increases slightly in the long isoflurane group as well. This spectral organization continues in general through the 2.75 h time point, while a gradual increase in the high-band frequencies (0.15–0.3) beginning to occur in both groups. At the 3.25 h time point, the power spectra of the two groups come close to convergence and evolve similarly throughout the final five time points. At 3.75 h, a strong peak begins to emerge at ~0.18Hz in both short and long isoflurane groups. By the 4.25 h time point, the ~0.18Hz peak dominates the spectra. This peak remains dominant throughout the remaining time points for both groups. Mean spectral data at the 4.25 h time point in the long isoflurane group were plotted for both the S1 cortex signal and the whole brain signal in Figure 2, indicating that the ~0.18Hz peak was specific to local cortical activity.

The average power and squared error of the mean (SEM) for the low-band, high-band, and broadband spectra were plotted in Figure 3 for both experimental groups. For low-band total power (Figure 3, left), statistical differences exist between the short and long isoflurane groups at 1.25 h ($p = 0.0003$), 1.75 h ($p = 0.0036$), and 2.75 h ($p = 0.0022$). Low-band spectral power values become more similar at 3.25 h and finally converge at 3.75 h. A similar trend is seen in the high-band power (Figure 3, center); however, average power values for the first time point (0.75 h) are more similar than in the low band; following the first time point there is an "unzipping" of high-band power data values until the 3.25 h time point, where the values "re-zip". Statistically significant differences were found for the same time points, 1.25 h ($p = 0.0049$), 1.75 h ($p = 0.0129$), and 2.75 h ($p = 0.0164$), as seen in the low band power. Broadband power (Figure 3, right) reflects a combination of low-band and high-band values; naturally, a similar trend is seen as in the previous two cases, although statistical differences between the short and long term isoflurane groups are also found at the 2.25 h time point ($p = 0.0001$) in addition to the 1.25 ($p = 0.0001$), 1.75 ($p = 0.0138$), and 2.75 ($p = 0.0017$) h time points. Qualitatively, the short isoflurane group appears to have greater power throughout all time points in the high-band and broadband ranges as compared with the long isoflurane group; however, SEM increases as the mean power increases and diminishes the statistical significance of differences between the two groups.

Peak power, peak location, center of spectral mass (CoM), and bilateral S1 functional connectivity were plotted in Figure 4 for both experimental groups. No statistically significant differences were found between the short and long isoflurane groups for CoM calculations (Figure 4, top left) or the frequency location of the maximum spectral power (Figure 4, bottom right). Maximum power occurring in the broadband spectrum (Figure 4, bottom left) is significantly different between the short and long isoflurane groups at 1.25 ($p = 0.0078$), 1.75 ($p = 0.0006$), and 2.75 ($p = 0.0103$) h. While mean maximum power appears greater in the short isoflurane group than the long isoflurane for most time points, SEM increases substantially as mean maximum spectral power increases, resulting in overlap in the error bars.

Intra-group analysis—Functional metrics were also evaluated on an intra-group basis (Table 2), assessing their evolution as a result of both time since isoflurane discontinuation and total duration under dexmedetomidine. Early time points (0.75–3.25 h) were compared with late time points (3.75–5.75 h) for each functional metric. Qualitatively, the short isoflurane group's low-band power showed a slight trend towards increasing power over the 5 h recording duration; however, comparing early data with late data did not reveal a significant difference. The long isoflurane group had a more dramatic increase in low-frequency power as a function of scanning time; a significant difference between early and late time points in long isoflurane low-band power was calculated ($p = 5.84 \times 10^{-8}$).

Short and long isoflurane high-band power displayed a strong increase as time under dexmedetomidine anesthesia increased, with statistically significant differences between early and late data in both experimental groups (short, $p = 0.0008$; long, $p = 2.8 \times 10^{-8}$). Much of this increasing power in the high-band data is a result of the appearance of a high-powered ~0.18Hz peak in both groups occurring around the 3.75 h time point (see Figure 1). Similarly, in the broadband power, data for both short and long isoflurane groups displayed

a pattern of increasing power over the duration of the scanning session, with both groups having highly significant differences between early and late data (short, $p = 2.23 \times 10^{-11}$; long, $p = 5.81 \times 10^{-5}$).

Intra-group analysis of center of spectral mass data revealed minor shifts over the duration of the experiment in both experimental groups (Figure 4, top left), but neither shift was significant after multiple-comparison correction. The maximum value of broadband spectral power increased significantly in both the short and long isoflurane groups over the experiment's duration (Figure 4, bottom left); both experimental groups confirmed a statistically significant shift in data from the first half of the experiment to the second (short, $p = 5.57 \times 10^{-6}$; long, $p = 0.0035$). Finally, the specific frequency location of the maximum spectral power also has a general trend of shifting towards the higher frequencies as the time under dexmedetomidine increases in both experimental groups (Figure 4, bottom right). Only the long isoflurane data exhibited a statistically significant shift in location of the maximum spectral power ($p = 0.035$).

Seed based functional connectivity

Inter-group analysis—Bilateral connectivity of the S1 cortex was evaluated for all rats and scans. There was a significant difference in functional connectivity (Figure 4, top right) between the short and long term isoflurane groups at only the 0.75h time point ($p = 0.0187$). While no other time points showed a significant difference in connectivity, convergence of mean connectivity values does not occur until the 2.25 h time point.

A visual example of functional connectivity over time is shown in Figure 5 (top). The resulting maps represent the correlation between a time course derived from the left S1 cortex and all other voxels within this coronal brain slice. In this example depicted in Figure 5 (long isoflurane – rat 7), functional connectivity generally increases as dexmedetomidine sedation times increases.

Connectivity between the average signal from the whole brain and each voxel in the brain was also evaluated for each rat and scan to determine anesthetic influences on whole brain connectivity. Whole brain mean connectivity was generally stronger for all data points from the short isoflurane data as compared with the long isoflurane data; however, significant differences were only confirmed at the 0.75 ($p = 0.0319$) and 1.75 ($p = 0.0292$) h time points. This is likely due to increased SEM values at higher mean power (Figure 5, lower right).

Intra-group analysis—Short isoflurane connectivity shifts throughout the duration of experiment but not in a monotonic fashion; SEM of recorded connectivity values increased significantly in the last 2 h of data collection. There is no significant evolution of short isoflurane functional data over the duration of the experiment. Long isoflurane connectivity increased consistently and significantly throughout the experimental duration ($p = 0.0002$).

Functional connectivity's relationship to low-band power

Total low-band spectral power (0.05–0.149 Hz) is plotted versus bilateral functional connectivity for both experimental groups in Figure 6. Linear regression of the short

isoflurane data did not reveal linearity or significance (Figure 6, left). Long isoflurane data did indicate a linearly significant relationship between low-band power and connectivity ($R^2 = 0.2635$, $p = 3.42 \times 10^{-6}$; Figure 6, right). A relationship between high-band power and functional connectivity was not significant in either experimental group. The relationship between broadband power and functional connectivity is significant in the long isoflurane data ($p = 0.0345$), but not in the short isoflurane data. A summary of these results can be found in Table 3.

Spatiotemporal dynamics

The template resulting from spatiotemporal dynamic analysis manifested in one of two forms: largely spatially unlocalized high and low correlations spread sporadically throughout the brain (Figure 7, top row – no coordinated spatiotemporal dynamics) or propagating waves of activity moving from the lateral cortex (S2) towards the medial cortex (M1) (Figure 7, bottom row – coordinated cortical spatiotemporal dynamics). The latter dynamic pattern matches what has been previously observed in the rat cortex under normal functional conditions; these spatiotemporal patterns are thought to contribute to functional connectivity observed between spatially distinct brain regions (29,31).

A second output of spatiotemporal dynamic analysis is a plot of mean spatial correlation versus the defined template. This correlation incidence analysis reveals patterns of activity that are spatially reproducible throughout the duration of the scan. Once this coordinated template is observed, it remains present throughout all subsequent scans in the study. Figure 7 shows a 4.5 s template generated from two scans occurring before the presence of strong spatiotemporal dynamics (top) and two scans occurring after the coordinated, reproducible spatiotemporal dynamics are present (bottom) in one rat (long isoflurane, rat 5). There is an obvious qualitative shift between the two states. Based on visualization, spatiotemporal dynamics are grouped as being either detectable or not detectable. The percentage of scans displaying coordinated cortical spatiotemporal dynamics is plotted for each time point and shown in Figure 8. Of note is that 50% of rats contain coordinated spatiotemporal dynamics by the 1.75 h time point in the short isoflurane group, while the 50% marker is not reached in the long isoflurane rats until the 3.25 h time point.

Physiological parameters

Heart rate, breathing rate, oxygen saturation, and body temperature over the duration of anesthesia were plotted in supplementary Figure 1. Physiological parameters all fell into acceptable ranges: heart rate – 300 ± 7.7 beats/min; breathing rate – 79.8 ± 5.1 breaths/min; oxygen saturation – 98.3 ± 0.23%; body temperature – 37.2 ± 0.13°C. Fifty-five (11 rats × five functional metrics) multivariate ANOVA regression analyses were performed between four physiological metrics (heart rate, breath rate, oxygenation, and temperature) and five functional metrics (CoM, maximum power, maximum location, functional connectivity, and band power) for all rats. 205 *P*-values (55 ANOVAs × four physiological parameters minus rats where specific physiology was not collected, see ANOVA section of methods) were obtained, and multiple-comparison correction was performed on the results. Three of 205 relationships resulted in significant correlations, which is less than the number expected by chance.

DISCUSSION AND CONCLUSION

To determine the effects of an anesthesia regimen consisting of isoflurane and prolonged dexmedetomidine use, we evaluated spectral components of functional BOLD activity, seed based functional connectivity, and the presence of spatiotemporal dynamics over a 5 h period of resting state fMRI scanning (0.75–5.75 h post dexmedetomidine bolus). Two experimental groups were used to compare and contrast the effects of increased periods of isoflurane use prior to functional imaging and possible effects of extended durations of dexmedetomidine use. The first experimental group was anesthetized using a short period of isoflurane, 30 min, followed by 5.75 h of dexmedetomidine anesthesia at a standard infusion dosage (5). The second experimental group's anesthesia regimen began with a long period under isoflurane, 3 h, followed by the standard dexmedetomidine dosing for 5.75 h. There were several significant differences between functional metrics in our two experimental groups within the first 2.75 h of scanning, but no significant differences were found between the two groups after 2.75 h. Both groups exhibited changes in the analyzed functional data as time under dexmedetomidine anesthesia (and time since use of isoflurane) increased. The variations in the functional metrics were more drastic in the long isoflurane group as compared to the short isoflurane group.

Recent studies have examined the differential effects of isoflurane and dexmedetomidine on resting state functional connectivity (12,13,16). Kalthoff *et al.* conducted a comprehensive investigation of each anesthesia separately, performing imaging under either 1.5% isoflurane or standard dexmedetomidine, and compared and contrasted the resulting functional state. Liu *et al.* identify effects of variable doses of isoflurane as it relates to functional activity. In this work we contribute an important missing link not provided by the two highly relevant studies mentioned above. The current work focuses on the effects of variable length of isoflurane dosing prior to the switch to dexmedetomidine and the time dependent, cumulative effects of isoflurane and dexmedetomidine by evaluating and comparing the resulting functional states. It is also important to note that the findings of this work are limited to the S1 cortex. Nasrallah *et al.* indicated differential neural effects of dexmedetomidine dependent upon the brain region evaluated, which were reported to be a function of α-2 receptor density (33). We focused on the S1 cortex, as it has been thoroughly characterized (2,6,9) in the rodent model and limits complexity from variable anatomical architecture.

The primary findings of this study suggest that increased durations of isoflurane use prior to functional imaging under dexmedetomidine anesthesia result in pronounced lingering effects of isoflurane that suppressed functional connectivity, spatiotemporal dynamics, and low frequency spectral power for multiple hours. Functional metrics from the long isoflurane data do not match those of the short isoflurane data until ~3.25 h following the cessation of isoflurane. Short isoflurane usage prior to functional imaging exhibits early signs of depression of functional connectivity and low-frequency power, but these effects diminish quickly, allowing for robust functional activity as early as 1.25 h following the cessation of isoflurane. Once the effects of isoflurane diminish there is a secondary effect, possibly arising from the use of dexmedetomidine anesthesia, manifesting as an evolving ~0.18 Hz peak in both the long and the short isoflurane data as time under dexmedetomidine

increases. Experimenters using the isoflurane/dexmedetomidine anesthetic regimen (5) for functional imaging should consider isoflurane sedation length prior to functional imaging when evaluating data and also be aware of the strong ~0.18 Hz peak that arises at the 3.75 h time point.

Parsing the effects of isoflurane from the effects of dexmedetomidine is a difficult task considering overlapping anesthetic influences in our experimental groups and the known lingering effects and interactions of both anesthesias; however, we can reasonably assume there are effects of both anesthesias based on the experimental results. Short isoflurane data have relatively consistent low-band power throughout the duration of the experiment, while low-frequency power in the long isoflurane data begins low and does not reach the power level of short isoflurane data until the 3.25 h time point. Similarly, functional connectivity in the short isoflurane data is relatively consistent throughout the duration of the experiment (although there is decreased mean and increased variation in the final hour of experimentation), while long isoflurane functional connectivity begins low and converges with the short isoflurane data around the 2.25 h time point. Evaluating the presence of highly coordinated patterns of spatiotemporal activity in each group reveals that spatiotemporal dynamics are present, on average, 1.5 h sooner in the short isoflurane data than the long isoflurane data. A final piece of the puzzle untangling the effects of isoflurane from dexmedetomidine lies in the relationship between low-band power and functional connectivity, which indicates there is no relationship between the two variables in the short isoflurane data but a linear relationship in the long isoflurane data. This relationship suggests depressed functional conditions (decreased low-frequency power and decreased functional connectivity) in the early portion of the long isoflurane experiment. Each of these occurrences suggests that short and long isoflurane data display differing functional signatures early in the experiment, which can only be attributed to the difference in isoflurane anesthetic duration.

The second portion of the results parsing the isoflurane effects from dexmedetomidine effects lies in the similarities between the two groups following the near spectral convergence at the 3.25 h time point. Both groups show a time locked evolution of high-band and broadband spectral power. Similarly, both groups show the presence of a strong ~0.18 Hz peak appearing at the 3.75 h time point following the cessation of isoflurane. Based on the known differential effects of isoflurane on the functional parameters, we infer that this time locked functional evolution may be attributed to the effects of the dexmedetomidine (or the generalized extended anesthetic condition) on either mechanical vascular properties, neural activity, or neurovascular coupling. Testing this hypothesis, pilot data were collected from rats where no isoflurane was used and only the initial bolus of dexmedetomidine was used to sedate the rats. Following initial sedation, dexmedetomidine infusion and imaging protocols were followed that were identical to the current study. Figure 9 shows the evolving power spectra for dexmedetomidine only rats. The ~0.18 Hz peak appears strongly at 4.25 h and dominates the low-frequency signal in a nearly identical manner to the two isoflurane experimental groups used in the current study. These pilot data further highlight the hypothesis that the emerging ~0.18Hz peak cannot be attributed to isoflurane and is likely associated with dexmedetomidine itself or the extended anesthetic condition (Figure 9).

We have gained two primary insights regarding the combined use of dexmedetomidine and isoflurane: (1) increased durations of isoflurane use prior to dexmedetomidine administration significantly influenced the spontaneous BOLD fluctuations, and (2) as the effects of isoflurane “wear off”, there were secondary functional activity effects that seemingly can only be attributed to long term dexmedetomidine use. Based on the two isoflurane lengths used in this study, we speculate that decreasing the time under isoflurane (<30 min) prior to the switch to dexmedetomidine would result in a further reduction in the duration of suppression of functional connectivity and spontaneous low-frequency activity following isoflurane cessation. Similarly, increasing the isoflurane dose beyond 3 h would likely result in an extended duration of suppression of the currently evaluated functional metrics.

Another interesting finding of this work relates to the functional significance of the two spectral bands (and the 0.18 Hz peak) that were evaluated. Low-band power (0.05–0.149 Hz) and bilateral functional connectivity increase in a coupled fashion in long isoflurane data, suggesting the functional relevance of this BOLD band. In contrast, the high-band power does not show any relationship to functional connectivity (a known neural correlate); the unexpected emergence of the high-amplitude ~0.18Hz peak does not result in a concurrent increase of functional connectivity. The ~0.18 Hz peak has been associated with the appearance of coordinated spatiotemporal dynamics (29), which in turn may be linked to infraslow electrical oscillations (4). The link between infraslow activity and the BOLD signal is strongly dependent on anesthesia (4), and may be related to the time variation observed in this study.

There was a significant difference in recorded physiological metrics between the pre- and post-3.75 h time points (corresponding to both the halfway point of the experiment and emergence of the ~0.18 Hz peak) for heart rate and oxygenation; however, all measurements fell into normal physiological ranges throughout the experiment. Oxygenation exhibited a sudden decrease of mean signal at the 4.75 h time point (supplementary Figure 1). Interestingly, most of the functional metrics recorded exhibited their greatest variance in the final three data points. Blood oxygenation is a primary influencer of the BOLD signal, and it is possible that the increased variance of the oxygenation was directly related to increased variance in the functional metrics.

In the refined dexmedetomidine paradigm of Pawela *et al.*, rodents responded to a tail pinch approximately 5.25 h following the dexmedetomidine bolus (5). The increased variance in the functional and physiological values obtained for the 4.75–5.75 h time points recorded in the current study likely reflect this increased level of wakefulness. Functional connectivity exhibited a greater decrease and greater variance in the final hour of experiment in the short isoflurane group as compared to the long isoflurane group. This higher variance, and lower mean connectivity, could possibly be attributed to the smaller sample size in the short isoflurane group; however, there were no significant differences between the two groups found in this time range.

Isoflurane is conventionally used for anesthetization before dexmedetomidine administration. The behavioral effects of volatile anesthetics typically wear off quickly

when administration is discontinued; however, isoflurane is also a potent vasodilator and the effects on the vasculature may persist after behavior has returned to baseline (34). Dexmedetomidine is a vasoconstrictor and may inhibit the cerebrovascular dilation induced by isoflurane. The inverse effects on vascular walls due to the change in anesthetics may cause unstable responses in neurovascular coupling during a certain period after the anesthetic switch (33). It is possible that the evolution of the ~0.18Hz BOLD peak is related to modulations in vascular tone. In 2010 our laboratory reported a study comparing functional connectivity measured with BOLD and cerebral blood volume (CBV) contrast (2). Interestingly, a ~0.2 Hz peak presents dominantly in the low-frequency spectrum for the CBV-weighted images, well before the 3.75 h critical time point discussed in this paper for the BOLD ~0.18Hz peak emergence. BOLD is a composite measure of cerebral blood flow, cerebral blood volume, and cerebral metabolic rate of oxygen, while an independent measure of CBV only accounts for changes in vascular volume. A vascular contribution at ~0.18Hz peak would be detected using a contrast mechanism heavily weighted towards the vasculature (CBV). Anesthesia may induce a time dependent increase in this vascular phenomenon, which can eventually be measured with BOLD contrast. An in depth evaluation of this ~0.18Hz peak deserves independent attention and an experimental design focused on probing its origin, and is a topic of future work.

This work focuses on the anesthetic protocols presented by Pawela *et al.* and Weber *et al.*, specifically the influences of the length of time under isoflurane prior to the switch to dexmedetomidine (5,10). Ideally anesthetized rodents should be in a condition as close to the “normal functioning” awake state as possible during fMRI; however, defining normal activity is not an easy task. In this work we have discovered that lingering effects of isoflurane have a significant effect on functional activity and persist after cessation of isoflurane at a length corresponding to the initial isoflurane anesthetic length. Similarly, we have uncovered an interesting phenomenon of a strong ~0.18Hz peak, which dominates the low-frequency spectrum beginning 3.75 h into the scanning period that should be explored in more depth. The potentially confounding factors associated with increased isoflurane sedation times could possibly be addressed with pharmacological intervention, change in dexmedetomidine dosage, or using an anesthesia other than isoflurane for induction; however, this is the topic of further work. Researchers should be aware that anesthetic agents may exhibit effects that vary over time and use caution when interpreting changes between groups or conditions that occur after different lengths of anesthetic administration.

Supplementary Material

Refer to Web version on PubMed Central for supplementary material.

Acknowledgments

NSF 1-R21NS057718-01, Scholarly Inquiry and Research at Emory (SIRE) Fellowship.

Abbreviations

BOLD blood-oxygen-level dependent

CNS	central nervous system
fcMRI	functional connectivity magnetic resonance imaging
S1	primary somatosensory cortex
CoM	center of mass
SGoF	sequential goodness of fit
SEM	squared error of the mean
EPI	echo planar imaging

References

1. Keilholz SD, Silva AC, Raman M, Merkle H, Koretsky AP. Functional MRI of the rodent somatosensory pathway using multislice echo planar imaging. Magn Reson Med. 2004; 52(1):89–99. [PubMed: 15236371]
2. Magnuson M, Majeed W, Keilholz SD. Functional connectivity in blood oxygenation level-dependent and cerebral blood volume-weighted resting state functional magnetic resonance imaging in the rat brain. J Magn Reson Imaging. 2010; 32(3):584–592. [PubMed: 20815055]
3. Pan WJ, Thompson G, Magnuson M, Majeed W, Jaeger D, Keilholz S. Broadband local field potentials correlate with spontaneous fluctuations in functional magnetic resonance imaging signals in the rat somatosensory cortex under isoflurane anesthesia. Brain Connectivity. 2011; 1(2):119–131. [PubMed: 22433008]
4. Pan WJ, Thompson GJ, Magnuson ME, Jaeger D, Keilholz S. Infraslow LFP correlates to resting-state fMRI BOLD signals. Neuroimage. 2013; 74:288–297. [PubMed: 23481462]
5. Pawela CP, Biswal BB, Hudetz AG, Schulte ML, Li R, Jones SR, Cho YR, Matloub HS, Hyde JS. A protocol for use of medetomidine anesthesia in rats for extended studies using task-induced BOLD contrast and resting-state functional connectivity. Neuroimage. 2009; 46(4):1137–1147. [PubMed: 19285560]
6. Williams KA, Magnuson M, Majeed W, LaConte SM, Peltier SJ, Hu X, Keilholz SD. Comparison of alpha-chloralose, medetomidine and isoflurane anesthesia for functional connectivity mapping in the rat. Magn Reson Imaging. 2010; 28(7):995–1003. [PubMed: 20456892]
7. Zhao F, Zhao T, Zhou L, Wu Q, Hu X. BOLD study of stimulation-induced neural activity and resting-state connectivity in medetomidine-sedated rat. Neuroimage. 2008; 39(1):248–260. [PubMed: 17904868]
8. Nakao Y, Itoh Y, Kuang TY, Cook M, Jehle J, Sokoloff L. Effects of anesthesia on functional activation of cerebral blood flow and metabolism. Proc Natl Acad Sci U S A. 2001; 98(13):7593–7598. [PubMed: 11390971]
9. Pawela CP, Biswal BB, Cho YR, Kao DS, Li R, Jones SR, Schulte ML, Matloub HS, Hudetz AG, Hyde JS. Resting-state functional connectivity of the rat brain. Magn Reson Med. 2008; 59(5): 1021–1029. [PubMed: 18429028]
10. Weber R, Ramos-Cabrer P, Wiedermann D, van Camp N, Hoehn M. A fully noninvasive and robust experimental protocol for longitudinal fMRI studies in the rat. Neuroimage. 2006; 29(4): 1303–1310. [PubMed: 16223588]
11. Guilfoyle DN, Gerum SV, Sanchez JL, Balla A, Sershen H, Javitt DC, Hoptman MJ. Functional connectivity fMRI in mouse brain at 7 T using isoflurane. J Neurosci Methods. 2013 Apr 15; 214(2):144–8. Epub 2013 Jan 31. 10.1016/j.jneumeth.2013.01.019 [PubMed: 23376497]
12. Kalthoff D, Po C, Wiedermann D, Hoehn M. Reliability and spatial specificity of rat brain sensorimotor functional connectivity networks are superior under sedation compared with general anesthesia. NMR Biomed. 2013
13. Liu X, Zhu XH, Zhang Y, Chen W. The change of functional connectivity specificity in rats under various anesthesia levels and its neural origin. Brain Topogr. 2012

14. Ferron JF, Kroeger D, Chever O, Amzica F. Cortical inhibition during burst suppression induced with isoflurane anesthesia. J Neurosci. 2009; 29(31):9850–9860. [PubMed: 19657037]
15. Antunes LM, Golledge HD, Roughan JV, Flecknell PA. Comparison of electroencephalogram activity and auditory evoked responses during isoflurane and halothane anaesthesia in the rat. Vet Anaesth Analg. 2003; 30(1):15–23. [PubMed: 14498913]
16. Hutchison RM, Mirsattari SM, Jones CK, Gati JS, Leung LS. Functional networks in the anesthetized rat brain revealed by independent component analysis of resting-state FMRI. J Neurophysiol. 2010; 103(6):3398–3406. [PubMed: 20410359]
17. Sommers MG, van Egmond J, Booij LH, Heerschap A. Isoflurane anesthesia is a valuable alternative for alpha-chloralose anesthesia in the forepaw stimulation model in rats. NMR Biomed. 2009; 22(4):414–418. [PubMed: 19003937]
18. Asano Y, Koehler RC, Kawaguchi T, McPherson RW. Pial arteriolar constriction to alpha 2-adrenergic agonist dexmedetomidine in the rat. Am J Physiol. 1997; 272(6 Pt 2):H2547–2556. [PubMed: 9227530]
19. Fukuda M, Vazquez AL, Zong X, Kim SG. Effects of the alpha(2)-adrenergic receptor agonist dexmedetomidine on neural, vascular and BOLD fMRI responses in the somatosensory cortex. Eur J Neurosci. 2013; 37(1):80–95. [PubMed: 23106361]
20. Nelson LE, Lu J, Guo T, Saper CB, Franks NP, Maze M. The alpha2-adrenoceptor agonist dexmedetomidine converges on an endogenous sleep-promoting pathway to exert its sedative effects. Anesthesiology. 2003; 98(2):428–436. [PubMed: 12552203]
21. Rehberg B, Xiao YH, Duch DS. Central nervous system sodium channels are significantly suppressed at clinical concentrations of volatile anesthetics. Anesthesiology. 1996; 84(5):1223–1233. discussion 1227A. [PubMed: 8624017]
22. Granholm M, McKusick BC, Westerholm FC, Aspegren JC. Evaluation of the clinical efficacy and safety of intramuscular and intravenous doses of dexmedetomidine and medetomidine in dogs and their reversal with atipamezole. Vet Record. 2007; 160(26):891–897.
23. Huttunen JK, Grohn O, Penttonen M. Coupling between simultaneously recorded BOLD response and neuronal activity in the rat somatosensory cortex. Neuroimage. 2008; 39(2):775–785. [PubMed: 17964186]
24. Sanganahalli BG, Herman P, Hyder F. Frequency-dependent tactile responses in rat brain measured by functional MRI. NMR Biomed. 2008; 21(4):410–416. [PubMed: 18435491]
25. Keilholz SD, Silva AC, Raman M, Merkle H, Koretsky AP. BOLD and CBV-weighted functional magnetic resonance imaging of the rat somatosensory system. Magn Reson Med. 2006; 55(2):316–324. [PubMed: 16372281]
26. Austin VC, Blamire AM, Allers KA, Sharp T, Styles P, Matthews PM, Sibson NR. Confounding effects of anesthesia on functional activation in rodent brain: a study of halothane and alpha-chloralose anesthesia. Neuroimage. 2005; 24(1):92–100. [PubMed: 15588600]
27. Biswal B, Yetkin FZ, Haughton VM, Hyde JS. Functional connectivity in the motor cortex of resting human brain using echo-planar MRI. Magn Reson Med. 1995; 34(4):537–541. [PubMed: 8524021]
28. Bullmore ET, Rabe-Hesketh S, Morris RG, Williams SC, Gregory L, Gray JA, Brammer MJ. Functional magnetic resonance image analysis of a large-scale neurocognitive network. Neuroimage. 1996; 4(1):16–33. [PubMed: 9345494]
29. Majeed W, Magnuson M, Keilholz SD. Spatiotemporal dynamics of low frequency fluctuations in BOLD fMRI of the rat. J Magn Reson Imaging. 2009; 30(2):384–393. [PubMed: 19629982]
30. Grigg O, Grady CL. Task-related effects on the temporal and spatial dynamics of resting-state functional connectivity in the default network. PLoS ONE. 2010; 5(10):e13311. [PubMed: 20967203]
31. Majeed W, Magnuson M, Hasenkamp W, Schwarb H, Schumacher EH, Barsalou L, Keilholz SD. Spatiotemporal dynamics of low frequency BOLD fluctuations in rats and humans. Neuroimage. 2011; 54(2):1140–1150. [PubMed: 20728554]
32. Carvajal-Rodriguez A, de Una-Alvarez J, Rolan-Alvarez E. A new multitest correction (SGoF) that increases its statistical power when increasing the number of tests. BMC Bioinformat. 2009; 10:209.

33. Nasrallah FA, Tan J, Chuang KH. Pharmacological modulation of functional connectivity: alpha2-adrenergic receptor agonist alters synchrony but not neural activation. Neuroimage. 2012; 60(1): 436–446. [PubMed: 22209807]

34. Ohata H, Iida H, Dohi S, Watanabe Y. Intravenous dexmedetomidine inhibits cerebrovascular dilation induced by isoflurane and sevoflurane in dogs. Anesth Analg. 1999; 89(2):370–377. [PubMed: 10439750]

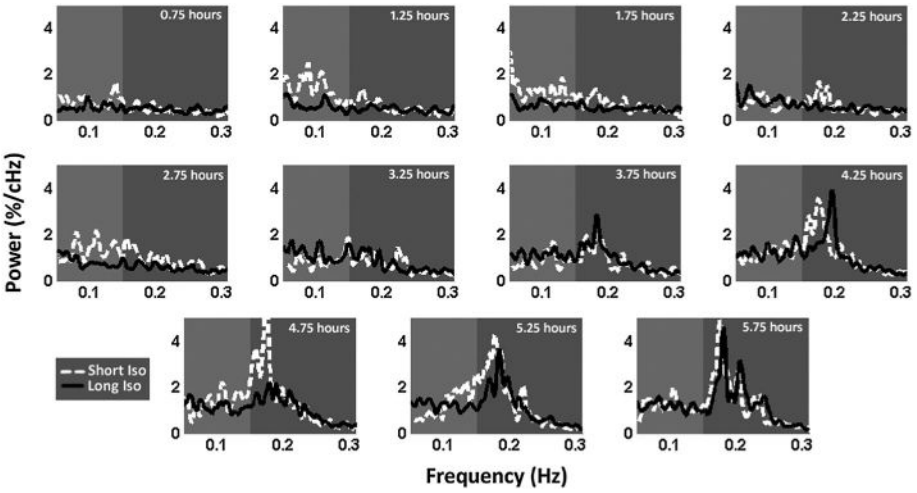

Figure 1.

Power spectrum evolution. Plots of average power spectra from the short isoflurane (30 min) group (four rats – dotted white line) and long isoflurane (3 h) group (seven rats – solid black line) followed by resting state imaging at 30 min intervals under a fixed dosage of dexmedetomidine for 5.75 h. Power spectra are derived from a time course generated from the left S1 cortex. Low-band power (0.05–0.149 Hz; light grey) increases at the 1.25 h time point in the short isoflurane group and does not increase in the long isoflurane to a similar level until the 3.25 h time point, when near convergence of the two groups' spectral signals occurs. At the 3.25 h time point, a strong ~0.18 Hz peak arises in both groups within the high-band data (0.15–0.3 Hz) and dominates the power spectra for the remainder of the functional scans. Both groups indicate a clear evolution of spectral information as time under dexmedetomidine (and time since isoflurane cessation) increases.

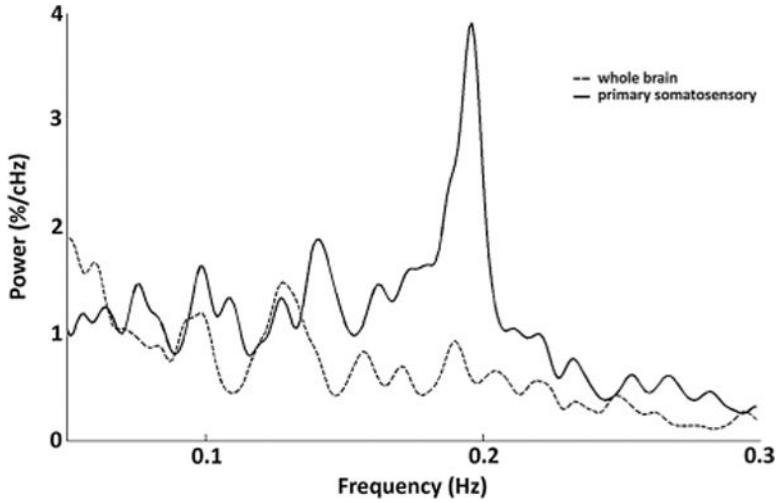

Figure 2.

Primary somatosensory cortex and whole brain spectra. The average group power spectra from the long isoflurane data at the 4.25 h time point are plotted for the both the S1 signal (solid line) and the global signal (dotted line). A strong peak at ~0.18 Hz dominates the low-frequency power spectrum of the S1 signal, but it is only minimally present in the whole brain spectra, indicating that this peak is a local phenomenon as opposed to a global one.

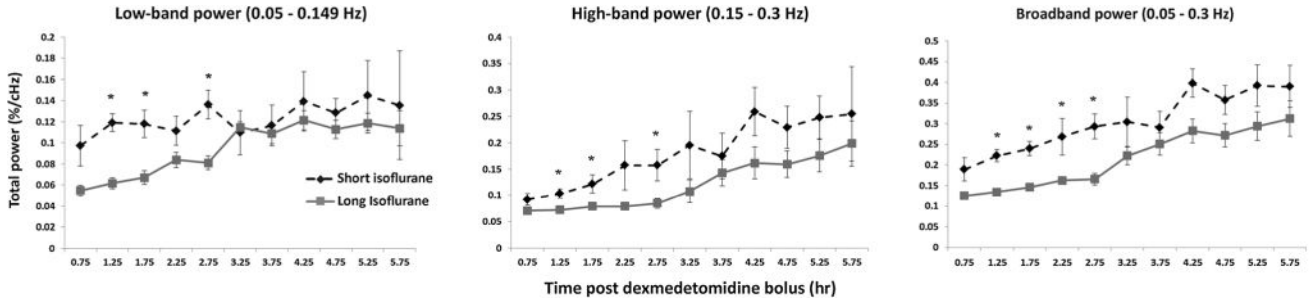

Figure 3.

Average power evolution. Summation of low-band power (left, 0.05–0.149 Hz), high-band power (middle, 0.15–0.3 Hz), and broadband power (right, 0.05–0.3 Hz) are shown for both the short (dotted) and long (solid) isoflurane groups. Mean and SEM values for each group are plotted for each time point. Significant differences are found between the short and long isoflurane groups in the low-band power at the 1.25, 1.75, and 2.25h data points, in the high-band power at the 1.25, 1.75, and 2.25 h data points, and in the broadband power at the 1.25, 1.75, 2.25, and 2.75h data points. Intra-group evaluations highlighting differences between early data and late data are calculated and presented in Table 2.

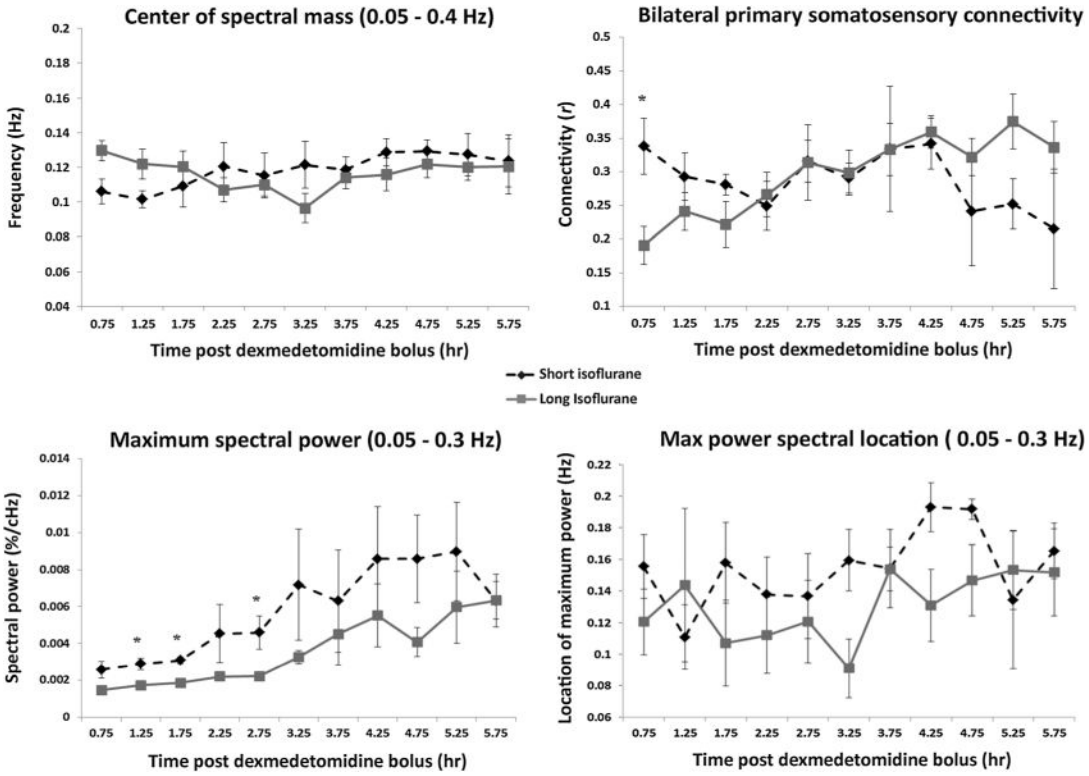

Figure 4.

Spectral characteristic and connectivity evolution. Average group values and SEM are plotted for center of spectral mass (top left), bilateral S1 connectivity (top right), maximum spectral power (bottom left), and the location of that maximum power (bottom right) for both the short (dotted line) and long isoflurane groups (solid line). No significant differences are found between the two groups for spectral CoM or for location of the maximum spectral power. Bilateral functional connectivity exhibits a significant difference between the groups at the 0.75 h time point followed by a convergence in connectivity data at the 2.25 h time point. Significant differences between maximum spectral powers are found at the 1.25, 1.75, and 2.75 h time points. Intra-group evaluations highlighting changes between early data and late data are calculated and presented in Table 2.

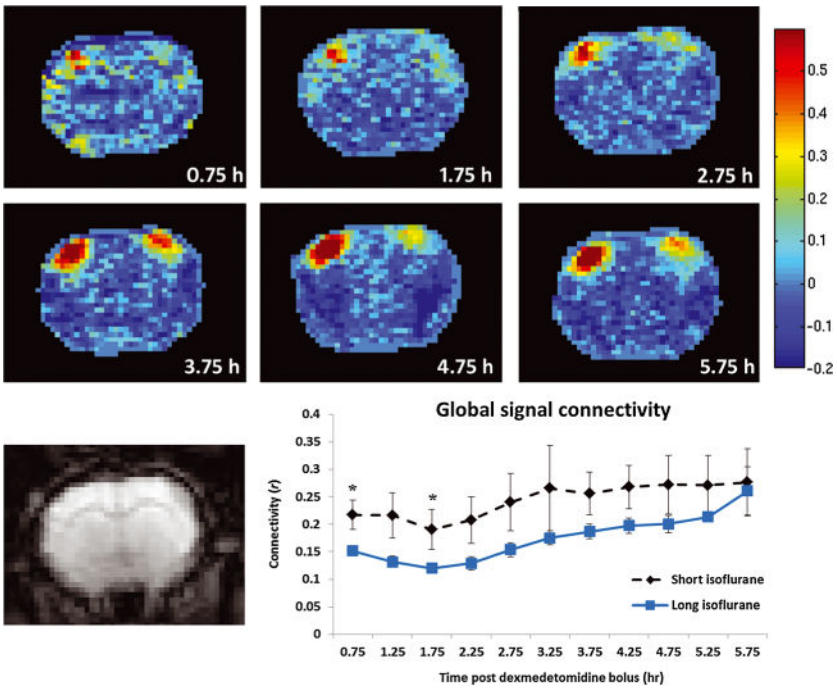

Figure 5.

Functional connectivity strength and spatial extent evolution. Top: correlation maps representing functional connectivity between left S1 and the rest of the coronal brain slice (coronal slice contains primary and secondary somatosensory cortices, the caudate putamen complex, and the primary motor cortices) as a function of time. The rat pictured is rat 7 from the long isoflurane group (chosen for display due to its similarity with the group correlation analysis). The strong correlation values in the left superior region represent correlation with the seed time course. High correlation values in the bilaterally symmetric region on the right side of the brain represent bilateral functional connectivity. As total time under dexmedetomidine increases functional connectivity becomes more prominent, until it reaches a semi-stable state around 3.75 h. Very little connectivity is evident before 2.75 h. Similar trends are apparent in the group analysis of long isoflurane data, as seen in the data in Figure 4. Bottom left: single-slice echo planar imaging (EPI) image corresponding to functional connectivity maps above. Bottom right: average correlation with the global signal is plotted as function of time for both short (dotted line) and long (solid line) isoflurane data with no global signal regression. Significant differences in global signal connectivity between the two groups are found at the 0.75 and 1.75 h time points.

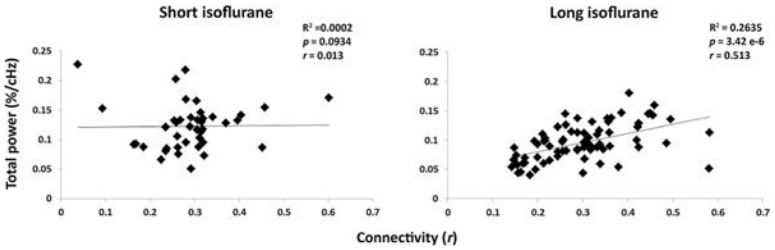

Figure 6.

Summation of low-band (0.05–0.149 Hz) power plotted against bilateral functional connectivity for the short (left) and long (right) isoflurane groups. There was no significant linear fit between short isoflurane and functional connectivity; however, a significant linear relationship was found between the low-band power and functional connectivity in the long isoflurane data.

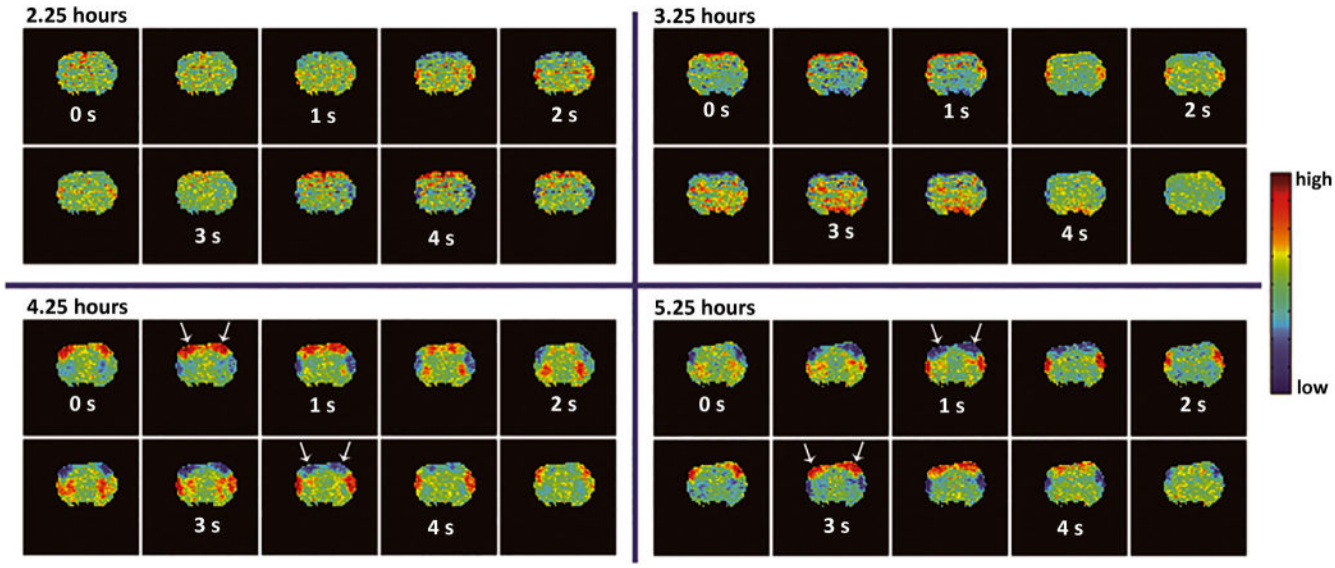

Figure 7.

Spatiotemporal dynamic evolution. Each of the four windows contains data from a single coronal brain slice containing the primary motor and S1 cortical brain regions. Spatiotemporal dynamic templates were generated from four time points of a single rat (2.25 h, 3.25 h, 4.25 h, and 5.25 h) from the long isoflurane group. These templates indicate repeating patterns of BOLD activity occurring in space and time. Detailed information regarding the formation of spatiotemporal dynamic templates can be found in the work of Majeed *et al.* (29). The top row indicates the state where no visible dynamics are present, while the bottom row shows the presence of coordinated cortical spatiotemporal dynamics. For this rat (long isoflurane, rat 5; chosen for display because of its similar timing to spatiotemporal group analysis for spatiotemporal dynamic data), spatiotemporal dynamics began at 3.75 h. High correlation values located on the edge of the brain at the 2.25 and 3.25 h time points are likely due to slight motion or breathing effects, and are present in the template as they represent the only pattern in that time point data that can be averaged together by the spatiotemporal dynamic algorithm.

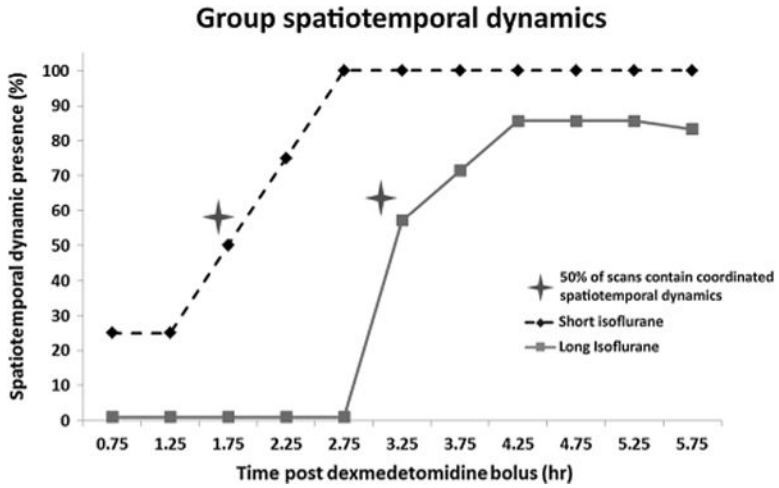

Figure 8.

Percent of rodents with coordinated cortical spatiotemporal dynamics present for each time point. Dynamics were grouped into the present and not present categories based on visual inspection of the dynamic template generated for each scan. Spatiotemporal dynamics are present in 50% of rats at the 1.75 h time point in the short isoflurane group (dotted line) and 50% of rats in the long isoflurane group (solid line) at the 3.25 h time point.

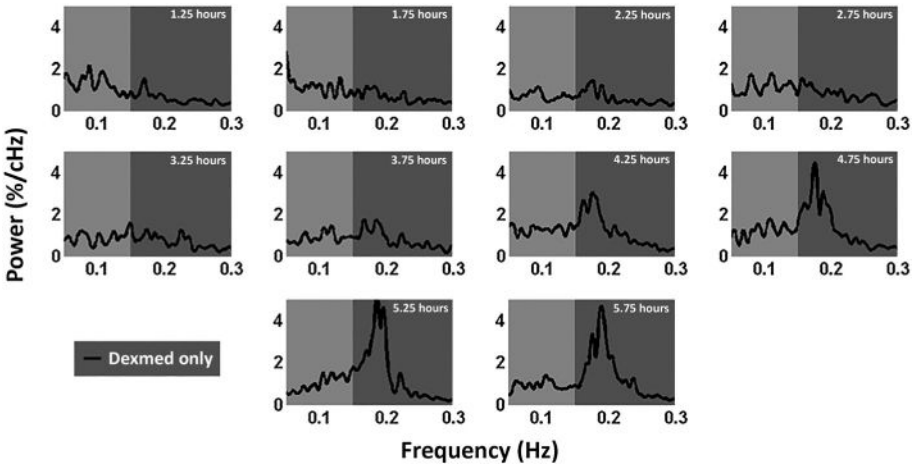

Figure 9.

Power spectra generated from a dexmedetomidine-only anesthetic paradigm. Five rats were injected with a bolus of dexmedetomidine while fully awake to induce the sedated state. Following sedation, standard dexmedetomidine infusion rates were used to maintain sedation. fMRI scans were collected at 30 min intervals for 5.75 h. This figure shows averaged power spectra at each time point obtained from the S1 cortex. Low-band power (0.05–0.15 Hz) remains relatively consistent throughout the study, while a strong ~0.18 Hz peak emerges around the 3.75 h time point and dominates the signal by the 4.25 h time point.

Table 1

Inter-group: *p*-values were calculated from Student's *t*-tests performed between the short and long isoflurane groups at each time point for each functional metric. The values highlighted in bold represent statistically significant differences between the groups that passed multiple-comparisons testing (SGoF) which indicated significance at $p < 0.0319$. Significant differences between the groups were found in functional connectivity, maximum spectral power, low-band, high-band, and broad-band power, and global connectivity (see Figures 3 and 4). Interestingly, no significant differences were found after the 2.75 h time point, suggesting the influences of the long isoflurane duration prior to functional imaging had dissipated by the 3.25 h time point

Time point (h)	0.75	1.25	1.75	2.25	2.75	3.25	3.75	4.25	4.75	5.25	5.75
Connectivity	**0.019**	0.283	0.245	0.746	0.976	0.874	0.992	0.685	0.250	0.110	0.178
Spectral CoM	0.035	0.113	0.490	0.353	0.682	0.132	0.666	0.383	0.365	0.370	0.420
Max. power	0.045	**0.008**	**0.0006**	0.079	**0.010**	0.114	0.572	0.348	0.044	0.412	0.185
Max. location	0.276	0.614	0.250	0.504	0.698	0.042	0.988	0.092	0.246	0.699	0.756
Low-band power	0.048	**0.0002**	**0.004**	0.078	**0.002**	0.771	0.691	0.474	0.359	0.319	0.617
High-band power	0.112	**0.005**	**0.013**	0.050	**0.016**	0.145	0.503	0.098	0.172	0.222	0.534
Broadband power	0.052	**0.0001**	**0.0001**	**0.0138**	**0.002**	0.149	0.414	0.035	0.123	0.151	0.310
Global connectivity	**0.032**	0.041	**0.029**	0.051	0.066	0.159	0.066	0.66	0.114	0.141	0.840

Table 2

Intra-group: *p*-values were calculated from Student's *t*-tests performed between all functional metrics comparing the 0.75–3.25 h time frame with the same metrics from the 3.75–5.75 h time points. All values highlighted in bold represent statistically significant findings passing multiple-comparison correction (SGoF), $p < 0.0345$. Long isoflurane data shows a significant evolution of functional metrics for five of eight functional metrics while short isoflurane data indicates a significant evolution of functional metrics for three of eight metrics

	Connectivity	CoM location	Max. power	Max. location	Low-band power (0.05–0.149 Hz)	High-band power (0.15–0.3 Hz)	Broadband power (0.05–0.3 Hz)	Global connectivity
Long ISO	**0.0002**	0.332	**5.57×10^{-6}**	**0.034**	**5.84×10^{-8}**	**2.8×10^{-8}**	**2.23×10^{-11}**	0.749
Short ISO	0.729	0.042	**0.003**	0.079	0.177	**0.0008**	**5.81×10^{-5}**	0.229

Table 3

R^2, p-values, and Pearson correlation values calculated indicating the relationship between total spectral power and functional connectivity. Significant linear relationships exist between long isoflurane data and functional connectivity in the low-band and broadband power spectra. No significant relationships exist between spectral power and functional connectivity in the short isoflurane data

		Low band (0.05–0.149 Hz)	High band (0.15–0.3 Hz)	Broadband (0.05–0.3 Hz)
Short isoflurane	R^2	0.0002	0.0059	0.0049
	p	0.9335	0.6339	0.6646
	r	0.0134	−0.0766	−0.0698
Long isoflurane	R^2	0.2635	0.0066	0.0614
	p	**3.42×10^{-6}**	0.4948	**0.0345**
	r	0.513 296	0.081 18	0.247 817